DEVICE FOR AUTOMATING *IN VITRO* CHARACTERIZATION OF LYMPHATIC VESSEL FUNCTION

A Thesis

by

SHRUTI RAJAGOPALAN

Submitted to the Office of Graduate Studies of
Texas A&M University
in partial fulfillment of the requirements for the degree of

MASTER OF SCIENCE

December 2004

Major Subject: Biomedical Engineering

DEVICE FOR AUTOMATING *IN VITRO* CHARACTERIZATION OF LYMPHATIC VESSEL FUNCTION

A Thesis

by

SHRUTI RAJAGOPALAN

Submitted to Texas A&M University
in partial fulfillment of the requirements
for the degree of

MASTER OF SCIENCE

Approved as to style and content by:

Christopher M. Quick (Chair of Committee)	John C. Criscione (Member)
Randolph H. Stewart (Member)	William Hyman (Department Head)

December 2004

Major Subject: Biomedical Engineering

ABSTRACT

Device for Automating *in vitro* Characterization of Lymphatic Vessel Function.

(December 2004)

Shruti Rajagopalan, B.E., Madras University, Chennai, India

Chair of Advisory Committee: Dr. Christopher M. Quick

The lymphatic system consists of a network of vessels which work to return the interstitial fluid back to the blood circulation. Individual units called lymphangions, segments of lymphatic vessels between two valves, pump cyclically to propel lymph. Lymphangions are similar to the heart in that they are sensitive to both preload and afterload. To describe the heart independent of preload and afterload, investigators developed the concept of time-varying elastance. We evaluated the applicability of this concept to lymphangions by analyzing preliminary data obtained from the bovine mesenteric vessels. We found that there were some limitations to the applicability of this concept to lymphangions, as there was a high degree of variability with respect to contraction strength and frequency of individual time-varying elastance curves. To better characterize lymphangion mechanics, we built a device which would enable real-time isobaric, isometric and isotonic experiments *in vitro*. We performed all three experiments on lymphatic vessel segments and obtained input and output pressures, output flow, instantaneous radii and wall tension. The characterization of the lymphangion using these

parameters can be the first step to simulate the behavior of a lymphatic vesssel and later the behavior of an entire lymphatic system.

To my parents and sister, Neethi, who have provided me with support through every phase of my life.

ACKNOWLEDGEMENTS

I am very grateful to my advisor, Dr. Christopher M. Quick, who provided this opportunity to me. He has helped me to get through all the difficulties I faced while writing this thesis. I am also grateful to Dr. Randolph H. Stewart who provided the data and many ideas for this work.

I would like to thank my friends, Anshul, Vidhya and Purna, who gave me their full support during the entire length of this thesis.

I would like to thank the lab members, Arun, Waqar and Ketaki, for their help. I would also like to thank Josh for helping me perform experiments which were crucial for writing this thesis.

I would like to thank my brother, Prashant and my roommates, Mini and Bharati. Lastly I would like to thank my friend Raghavendra.

TABLE OF CONTENTS

Page

Page

LIST OF FIGURES

Page

Page

CHAPTER I

INTRODUCTION

1.1 Building blocks of the lymphatic system

The lymphatic system consists of a network of vessels that returns interstitial fluid and protein to the blood circulation. The failure of the lymphatic system is one of the causes for a condition called edema, an inappropriate accumulation of fluid in tissue occurring when microvascular filtration into the tissues exceeds the fluid removal rate by the lymphatic system. Pathological conditions such as inflammation, invasion of parasites or bacteria and cancer can cause edema, which in turn can be fatal (18). There are currently limited treatments for edema.

The lymphatic system consists of units called lymphangions, the segments of lymphatic vessels between two adjacent unidirectional valves (11). Under normal conditions, interstitial fluid (called lymph once in the lymphatic system) must be propelled up a pressure gradient. There are several forces that act in this propulsion of lymph up a pressure gradient. Lymphatic vessels can be compressed by external forces (extrinsic pump), but can also cyclically contract (intrinsic pump). However, under some conditions, like extreme edema or changes in position, the pressure gradient can reverse. In this case, lymphatic vessels may act more like conduits.

This thesis follows the style and format of the *American Journal of Physiology-Heart and Circulatory Physiology*.

1.2 Similarity to the heart

Lymphangion behavior resembles that of the heart in many ways. Lymphangions expand and contract cyclically, like the heart, making the lymphangion pump fluid against a pressure gradient. Lymphangion output is sensitive to transmural pressure, and therefore both preload and afterload (5, 6). Due to its functional similarities to the heart, investigators have described it in terms similar to the heart. Terms like systole, diastole, stroke volume and ejection fraction have been used to characterize lymphangion behavior (1, 2), and have dominated the recent view of how lymphangions behave.

1.3 Pressure-volume loops for the heart

Otto Frank first described a pressure-volume relationship for the heart in 1899 (8), which has become common means for characterizing ventricular function. The form of the pressure-volume loop reflects four stages of the cardiac cycle. They are ventricular filling, isovolumic contraction, ejection and isovolumic relaxation. The maximum volume obtained at the end of relaxation is the end-diastolic volume (EDV) and the minimum volume obtained at the end of contraction is the end-systolic volume (ESV). Because developed pressure is very sensitive to EDV, a single pressure-volume loop is not sufficient to describe the contractile state of the heart. Suga et al. noted that the end systolic pressure-volume relationship (ESPVR) was particularly stable (17). They maintained that at a given contractility, the ESPVR remains relatively constant. The ESPVR is more linear than the end-diastolic

pressure-volume relationship (EDPVR). Figure 1 shows an illustration of the characteristics of pressure-volume loops.

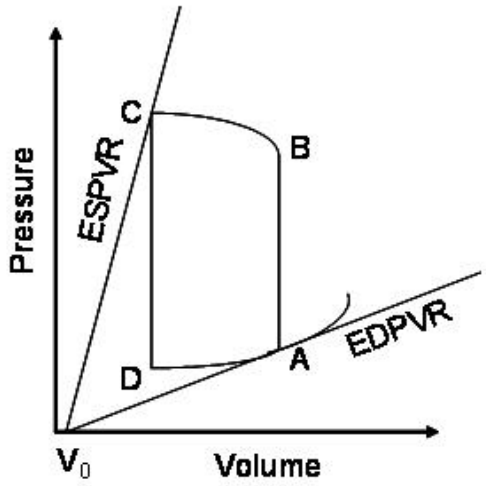

Figure 1: Pressure-volume loops for the heart. Point A represents the end diastolic phase, Point B is the end of the isovolumic contraction phase, Point C is the end systolic phase and Point D is the end of isovolumic relaxation.

1.4 Indices of contractility for the heart

A contractility index independent of preload and afterload and heart rate has been much in demand for clinical purposes in order to asses cardiac function independent of vascular function. Contractility is roughly defined as the strength of the ventricular contraction, but has been the subject of much discussion. Commonly used indices, such as ejection fraction, are affected by preload and afterload and hence are not very reliable.

One of the most common indices of contractility used by research scientists is E_{max}, the slope of the ESPVR. It has been used as the index of contractility since it

changes with changes in force generated by cardiac muscle, and is insensitive to preload. There has been debate about its use as well (15).

1.5 Instantaneous pressure-volume ratio for the heart

The time-varying elastance, E(t), in its most basic form is the instantaneous ratio of chamber pressure and volume

$$E(t) = \frac{P(t)}{(V(t) - V_0)} \tag{1}$$

where P(t) is the instantaneous intraventricular pressure, V(t) is the instantaneous intraventricular volume and V_0 is the theoretical volume at zero pressure. This equation defines the pressure-volume ratio at any time in one cardiac cycle. Figure 2 shows a schematic of a typical instantaneous pressure-volume ratio curve for a control and an enhanced contractile state. The figure 2A shows the effects of progressively increasing systolic pressure keeping the end diastolic volume constant. The figure 2B shows the effects of progressively increasing end diastolic volume keeping the systolic pressure constant. The figure 2C shows the effects of increased and decreased contractile state of the heart. The center line signifies the control contractile state.

A

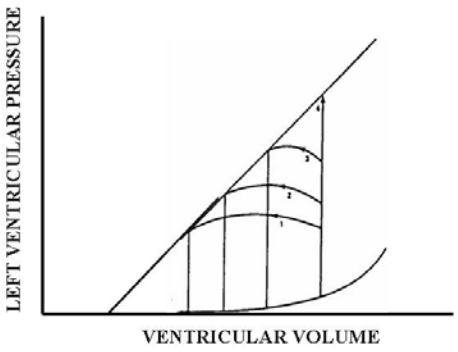

B

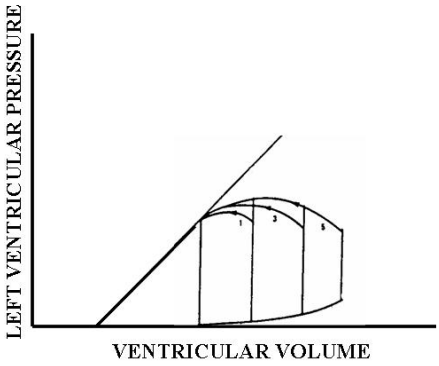

C

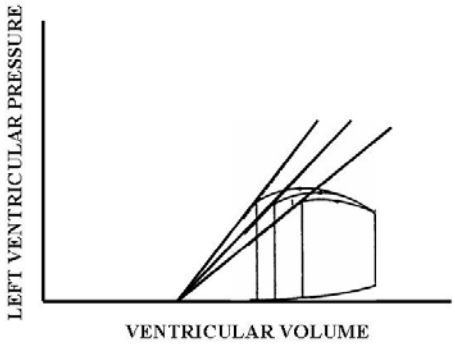

Figure 2: Instantaneous pressure-volume ratio curve for a control and an enhanced contractile state. The figure A shows the effects of progressively increasing systolic pressure keeping the end diastolic volume constant. The figure B shows the effects of progressively increasing end diastolic volume keeping the systolic pressure constant. The figure C shows the effects of increased and decreased contractile state of the heart. The center line signifies the control contractile state.

The peak value of E(t), E_{max}, increases and the time to the peak, T_{max}, decreases as the contractility increases. However, it was noticed that even though these values changed, the shape of the curves were similar. Suga et al. (20) normalized the curves to compare the shape of the ratios under different contractile states:

$$E_N = \frac{E(t)}{E_{\max}} \tag{2}$$

$$t_N = \frac{t}{t_{\max}} \tag{3}$$

where E_N is the normalized elastance, E(t) is the instantaneous elastance, E_{max} is the maximum value of E(t), t_N is the normalized time period, t is the time, and t_{max} is the time taken to reach E_{max}.

Figure 3 shows a schematic of a normalized elastance curve. Elastance curves derived from pressure-volume relationships at different preloads fell roughly on the same curve, illustrating the insensitivity of E(t) to changes in preload(19). Similar studies showed that E(t) was insensitive to changes in afterload (19).

Because E_{max} and T_{max} were insensitive of wide variations in preload and afterload conditions, and is sensitive to changes in contractile state, E_{max} could be employed as an index of contractility. Palladino et al. said that the pressure-volume relationship is not constant, but is sensitive to flow; an isovolumic analytical model of the left ventricle is thus a better way to define ventricular contractility (15). But even with this challenge,

time-varying elastance continues to be a popular characterization of basic cardiac behavior for modeling purposes.

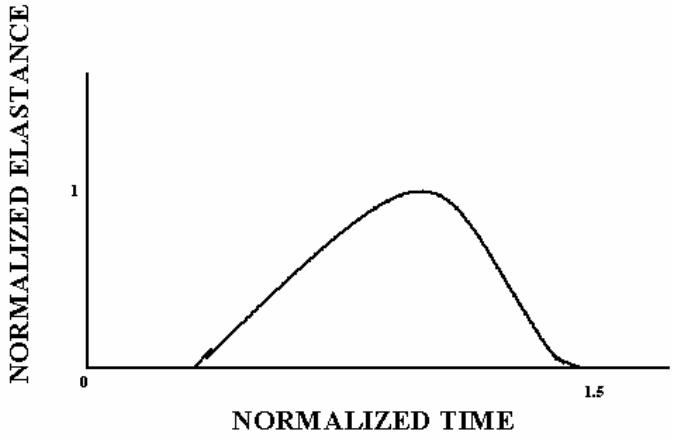

Figure 3: Normalized elastance curves for a ventricle. The time was divided by the time period such that the maximum time was made 1.5 and the maximum contractility was made unity.

1.6 Pressure-volume relationships in lymphatic vessels

Li et al. and Benoit et al. have applied descriptions of the heart to the lymphangions and obtained pressure-volume loops (2, 13). Figure 4 shows one pressure-volume loop for a lymphatic vessel obtained by Benoit et al. (2). The figure shows two phases of systole and four phases of diastole. Phase 1 of systole (A-B) is characterized by a rapid increase in pressure and decrease in volume. Point A defines the end-diastolic volume and point B, the peak pressure corresponding to this volume. Points B-C denotes the phase 2 of systole, where point C is the end-systolic volume and pressure. Points C-D show the phase 1 of diastole, which is a period of

isovolumic relaxation. Point D denotes the end of isovolumic relaxation. Phase 2 of diastole (D-E) is a phase of rapid filling. Point E denotes the end of rapid-filling. Phase 3 of diastole (E-F) is the slow-filling period and point F denotes the end of slow-filling. The last phase of diastole is phase 4 (F-A), which is a period of active-filling from the upstream lymphangion. The last phase of diastole brings us back to systole, starting another contractile cycle. According to their results, diastole extends for much longer than systole. Figure 5 illustrates the response at various transmural pressures obtained by Li et al. (13). The pressure-volume loops obtained for the lymphangions had a nearly linear end systolic pressure-volume relationship (ESPVR) and an exponential end diastolic pressure-volume relationship (EDPVR).

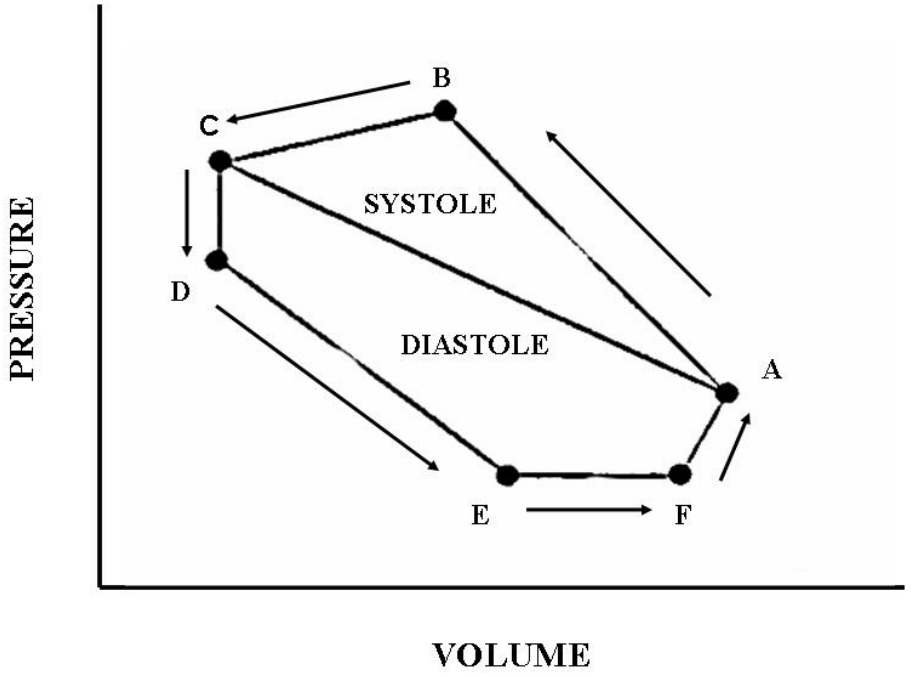

Figure 4: Pressure-volume loop for a lymphatic vessel. Points A-C represent the systolic phase and Points C-A the diastolic phase. Digitized and reproduced from Benoit et al., Am J Physiol 257: H2059-2069, 1989 (2).

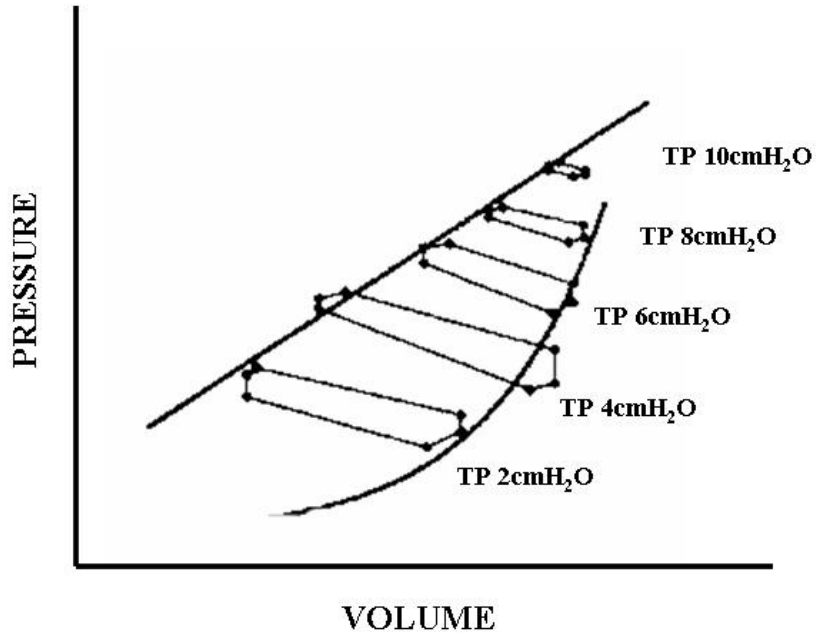

Figure 5: Pressure-volume loops at various transmural pressures for a lymphatic vessel. The pressures were varied from 2 cmH_2O to 10 cmH_2O. Digitized and reproduced from Li et al., Microvasc Res 56: 127-138, 1998 (13).

1.7 Heart as a pump

The heart functions as a pump that must deliver blood throughout the body and hence has to generate alternately high pressures and high flows. Researchers through the ages have been making the analogy of the heart as a mechanical pump. Elzinga and Westerhof have described the heart quantitatively like a mechanical pump (21). Figure 6 is a schematic illustrating the relationship between the mean left ventricular pressure and cardiac output. It can be inferred from the figure that at high pressures, flow is low and large changes in flow can be achieved with slight changes in pressure. Similarly, at high flows, the pressure is small and large pressure changes are required for even small changes in flow. Thus, the heart acts as a pressure source

when beating against high loads, and as a flow source when acting against low pressures. These investigators also studied the effects of a change in contractility of the heart. They found that at lower contractility (as in cases of heart failure), the heart functions primarily as a pressure source with the flow extremely sensitive to pressure.

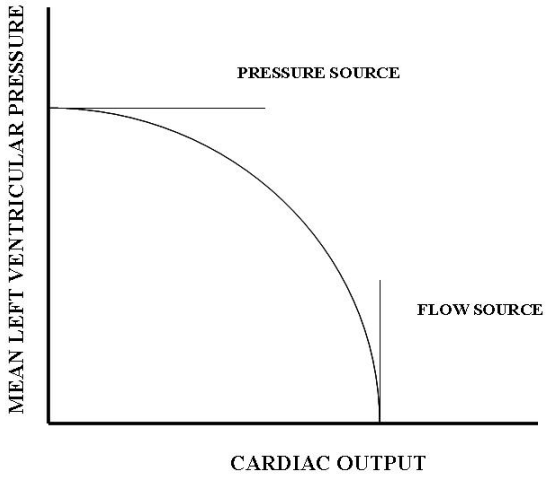

Figure 6: Relationship between the mean left ventricular pressure and the cardiac output. At high loads the heart acts as a pressure source and at low pressures, it acts like a flow source. Digitized from original reference in McDonald's Blood Flow of Arteries, Oxford University Press, 1998 (21).

1.8 Lymphangions as pumps

Figure 7 illustrates the relationship between the lymph flow rate and the outflow pressure obtained from intact lymphatic vessels of the lung in unanesthetized sheep (4). They measured the flow rate at the cannulated vessel held at different heights above a baseline. As the outflow pressure increases, lymph flow decreases. They showed that the cannulated lymph vessels generated high pressures and referred to the lymph vessels as exhibiting behavior that can be described by an "effective driving pressure" and an

"effective resistance". The reason that their results do not show the typical pump behavior in figure 6 (lymphatic vessels showed a linear relationship between the outflow pressure and lymph flow), could be that this behavior is an average behavior of many lymphangions and includes the effects of an internal resistance to lymph flow. It is the inability to separate pump and resistive effects that informs the direction of the present work.

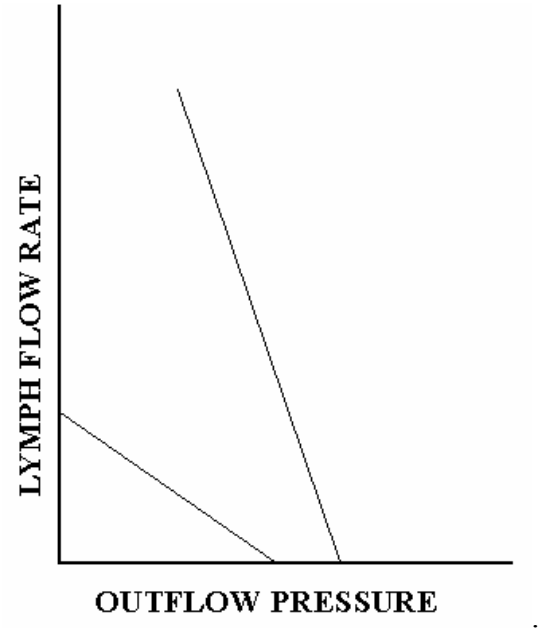

Figure 7: Effect of outflow pressure on lung lymph flow. As the outflow pressure increases, the lymph flow decreases. Digitized and reproduced from Drake et al., J Appl Physiol 58: 70-76, 1985 (4).

1.9 Isometric, isotonic and isobaric experiments

Researchers interested in characterizing cardiac muscle were able to build upon the work done to characterize skeletal muscle (14). In particular, multi-element models like those describing skeletal muscle have been adopted to study cardiac

muscle dynamics. Hefnor and Bowen used the three-element model, which is a variation of the two-element model of Hill (12). A further variation of this model was used by Brady (3). Parmley and Sonnenblick used a four-element model (16). Figure 8 shows the three model representations.

The use of all these models requires the assignment of numerical values to the various elements. To understand the relationships between various parameters of the models, the simplest model – the two-element model- is the most useful. The two-element model consists of a contractile element (CE) and a series element (SE) acted upon by a preload, as shown in figure 9. In a classical experiment on isolated muscle, a strip of muscle is first subjected to isometric contraction, followed by an isotonic contraction. The isometric contraction yields the maximum tension that can be developed by the muscle and the isotonic contraction yields the velocity of shortening of the muscle. In the isometric phase, when this system is stimulated, the CE will shorten, and to compensate this shortening, the SE will be stretched. When the contractile force developed by the CE becomes greater than that developed during stimulation, the CE undergoes isotonic contraction. When the isotonic contraction begins, the SE length stays constant. Thus the initial velocity of shortening of the whole muscle is equal to that of the CE.

To relate lymphatic vessel mechanics to its function, only isobaric experiments have been performed; classical means of characterizing muscular tissue (isometric and isotonic experiments) have not been performed. Furthermore, functional experiments on vessels *in vitro* have relied on isobaric boundary

conditions. No one has yet performed *in vitro* experiments with realistic, dynamic boundary conditions.

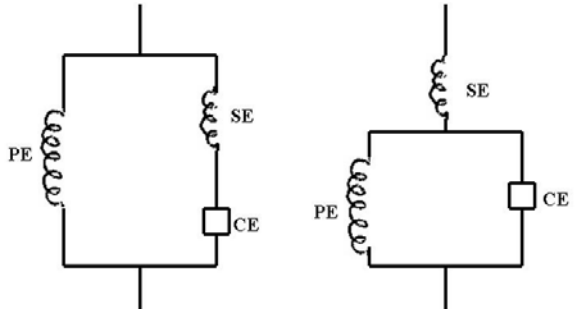

Figure 8: The three model representations. Investigators Hefnor and Bowen used these models to characterize cardiac muscle dynamics. Digitized and reproduced from original reference in Circulatory System Dynamics, Academic Press Inc., 1978 (14).

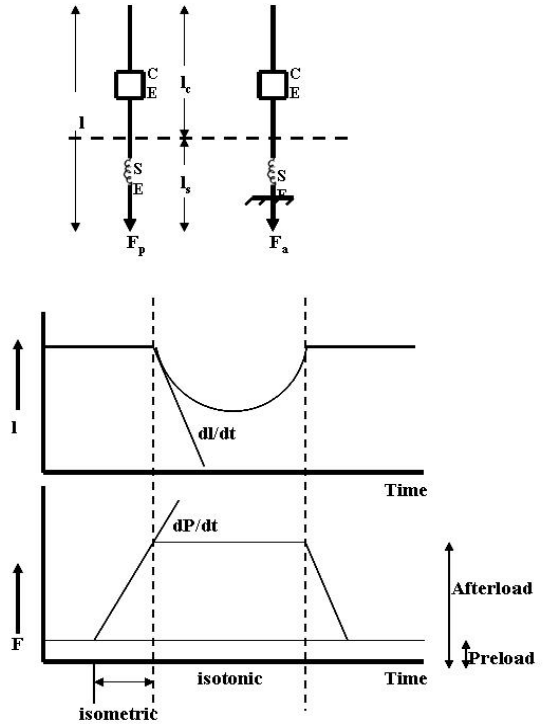

Figure 9: Procedure to derive properties of the contractile and series elastic elements. Digitized and reproduced from original reference in Circulatory System Dynamics, Academic Press Inc., 1978 (14).

CHAPTER II

GOALS FOR THE THESIS

2.1 Aims for device creation

2.1.1 To characterize the lymphangion independent of inlet and outlet pressures using the time-varying elastance concept

If the time-varying elastance concept can be applied to characterize the lymphangions, this would enable us to characterize the lymphangion independent of inlet and outlet pressures. The results of this analysis can be used to:

a) Form a basis for mathematical characterization.

b) Build a device which mimics actual lymphangions.

2.1.2 To create a device to study lymphatic vessel function

This device would have a negative feedback system to set pressures that dynamically controls transmural pressures in a lymphatic vessel to act like lymphangions characterized in objective 1.

2.1.3 To create a device to study lymphangion mechanics

The same device with a negative feedback would be used to conduct isometric, isotonic and isobaric experiments to study lymphangion mechanics.

2.2 Experimental set-up

The experimental set-up used to study lymphatic function will be explained in chapter III. The same set-up is used for studying lymphangion mechanics as well, but with a few additions and modifications. This will be described in chapter IV.

2.3 Analysis of this device

The performance of the device to study both lymphangion function and mechanics will be analyzed in chapter V. The outcome will be discussed in chapter VI, wherein the future directions will also be discussed.

CHAPTER III

APPLYING THE TIME-VARYING ELASTANCE CONCEPT TO LYMPHANGIONS*

3.1 Experimental set-up

As explained in chapter I, there are many similarities between the lymphangions and ventricles. To study lymphangion function, we decided to study the variables commonly used to study the heart. Post-nodal bovine mesenteric lymphatic vessels were placed in a tubular organ bath for these experiments. Figure 10 illustrates the experimental set-up.

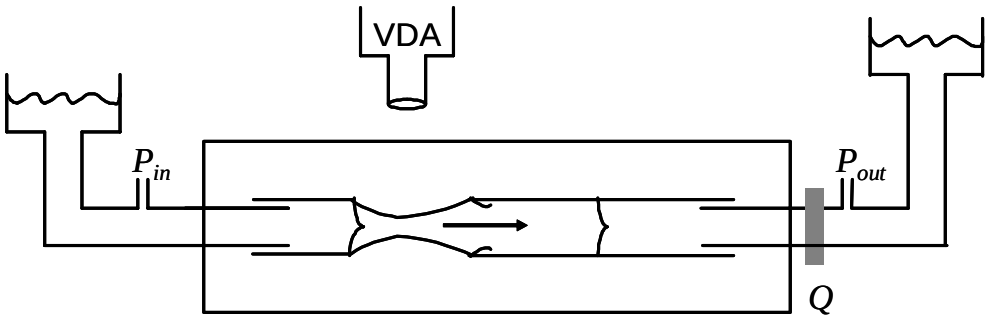

Figure 10: The experimental set-up to characterize isolated bovine mesenteric lymphangions. This set-up was used to measure the diameter of the vessel using the Video Dimension Analyzer (VDA), and to measure the inlet and outlet pressures using pressure transducers.

---

* Reprinted, with permission, from "Evaluating the time-varying concept for lymphangions" by Shruti Rajagopalan et. al., 2003. Proc. - IEEE/EMBS 25th Ann. Int. meet.. © 2003 IEEE.

Data for three vessels were recorded for analysis. The vessels were perfused with a balanced polyionic solution gassed with 95% O_2 – 5% CO_2 sufficient to maintain pH at 7.4. The length of the vessel segments were 4.2 cm. Transmural pressure was altered by setting the inlet and outlet pressures. Transmural pressure (P) is estimated by the formula:

$$P = \left[\frac{(P_{in} - P_{out})}{2} \right] - P_{ext} \tag{4}$$

where P_{in} is the inlet pressure, P_{out} is the outlet pressure and P_{ext} is the external pressure, which is set to 1 mmHg. Volume was calculated from radius assuming that the lymphangion maintained a uniform cylindrical shape during contraction,

$$V = \pi \cdot r^2 \cdot l \tag{5}$$

where r is the radius of the vessel and l is the length of the vessel. The radius of the vessel is obtained using a diameter tracking program developed from LabVIEW and IMAQ Vision components. Experiments were performed on three different vessel segments. One vessel had a single valve while the other two were valveless. The resulting flow was measured via a pressure drop across a coil of tubing with known resistance. For the third vessel, P_{in} and P_{out} were elevated at the same time, that is, the axial pressure gradient was zero and transmural pressure was varied.

Pressure-volume curves were recorded and elastances at different P were calculated using (1) and were plotted as a function of time. Maximum and minimum values of E(t), E_{max} and $E_{min,}$ respectively, were calculated from the data for

representative beats, and then normalized elastance, E′(t), was calculated using the equation:

$$E' = \frac{\left(E(t) - E_{\min}\right)}{\left(E_{\max} - E_{\min}\right)}. \quad (6)$$

Time was also normalized by the time period (*T*),

$$t' = \frac{t}{T} \quad (7)$$

where *t′* is resulting normalized time. The dead volume, V_o, in Eq. 1 was obtained from the pressure-volume plot, where the ESPVR intercepts the volume axis.

Sensitivity of elastance to peak pressure, mean pressure and flow were evaluated. Data from 4-5 representative cycles from each vessel were analyzed.

3.2 Data analysis

3.2.1 Normalized elastance

Classically, *E*(*t*) is used to describe contractility of the heart independent of preload and afterload. We used this concept to describe the lymphangions in similar terms. On analysis of data, however, we found that the time-varying elastance of lymphangions is not independent of preload and afterload. The data exhibited a high degree of variability, as shown in figure 11. Hence we normalized the elastance curves in order to determine if they show similar patterns, and thus able to be generalized in the form of a simple equation. Figure 12 illustrates elastance

normalized using Eq. 6 for a single vessel based on select pressure-volume curves shown in the figure 13. We can see that even though the curves are stable, they do not appear to be consistent; values of E_{max}, E_{min} and T vary. Figure 12 shows the curves after they have been normalized. The resulting normalized curves have nearly the same shape and pattern.

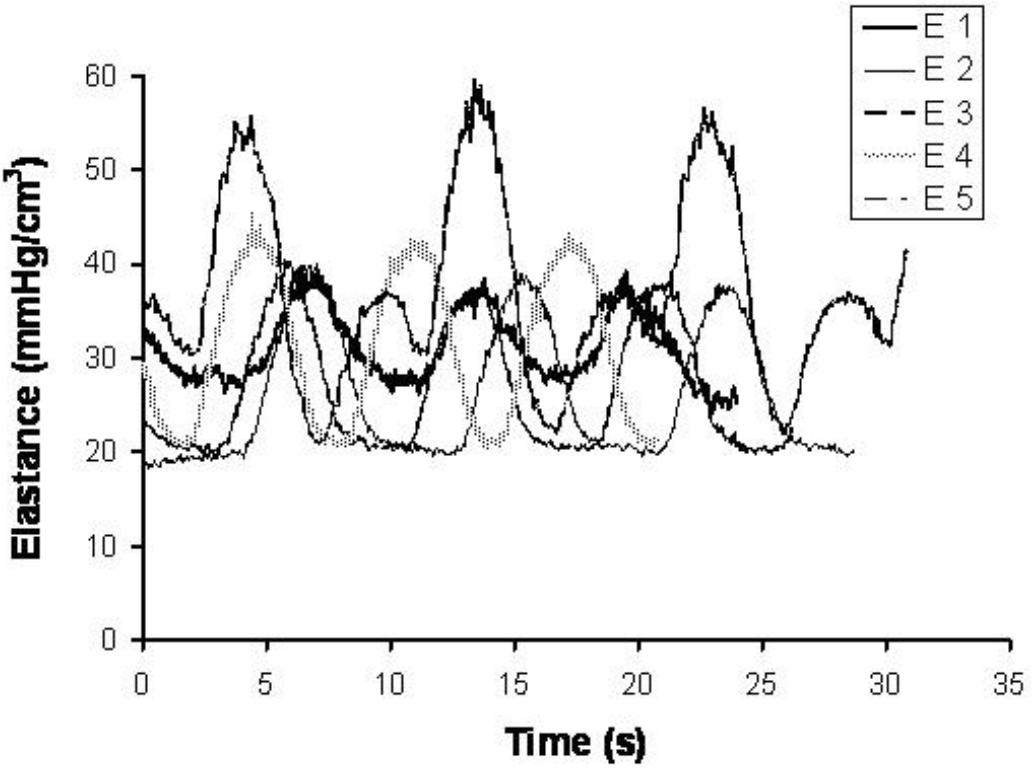

Figure 11: Elastance curves for five cycles of a single lymphangion at different transmural pressures. As we can see, the frequency of contraction, minimum and maximum elastances all vary for the five cycles.

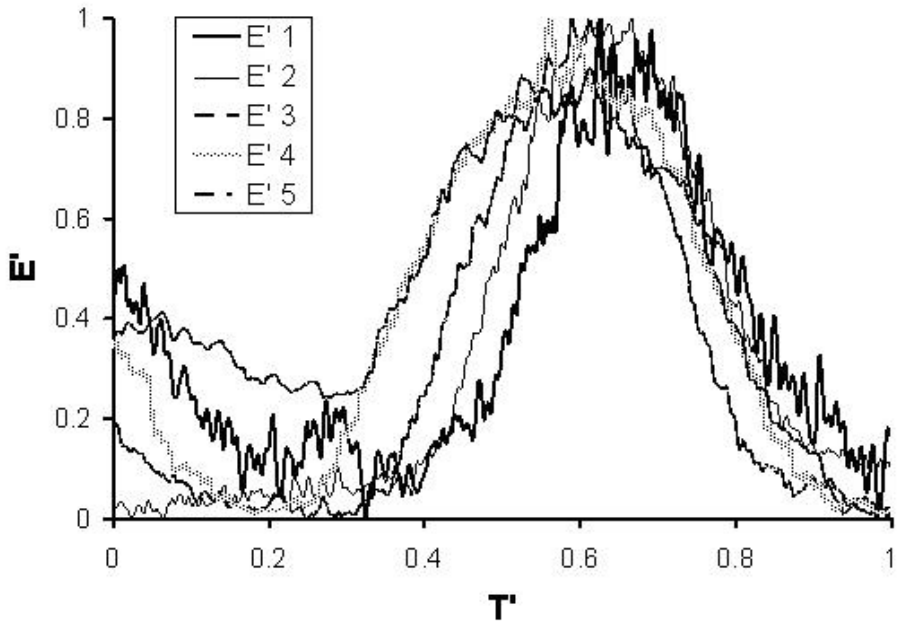

Figure 12: Normalized elastance curves. These curves were obtained by applying Eqs. 6 and 7 to the curves in figure 11.

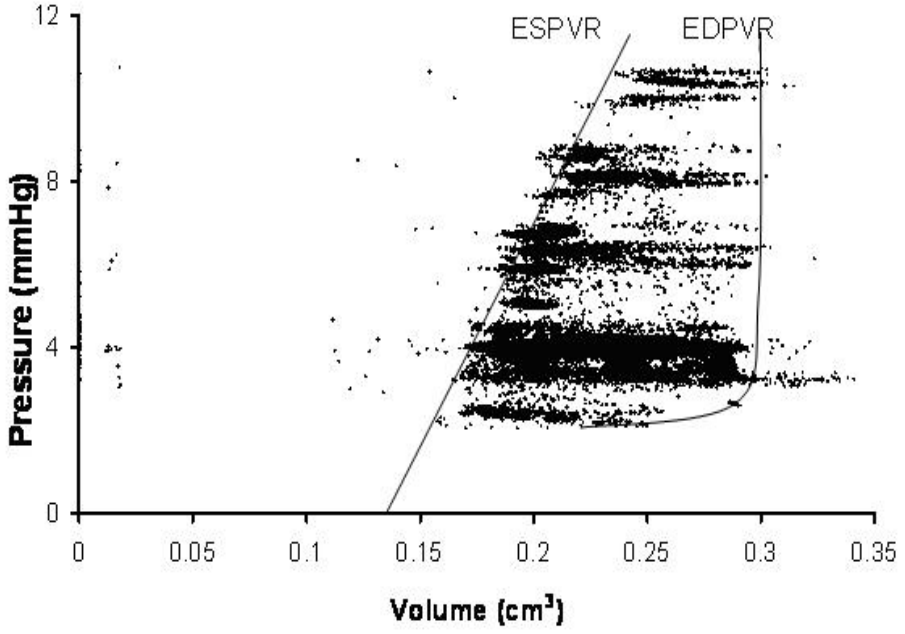

Figure 13: Pressure-volume curves for lymphangions. These are various points obtained from an experiment conducted on one lymphatic vessel. The end systolic pressure-volume relationship (ESPVR) and end diastolic pressure-volume relationship (EDPVR) were obtained by randomly picking the ESPVR of loops and connecting them.

3.2.2 Peak pressure vs E_{max}

Figure 13 shows the pressure-volume relationship for one lymphangion. Classically a ventricular pressure-volume relationship is derived from one contractile cycle, but the pressure-volume relationship for the lymphangion was more difficult to characterize. Not all loops started and ended at the same point. Hence, we analyzed the data and took from the data few pressure-volume loops which we thought were complete (starting and ending at the same point) and plotted the elastance curves. From each such curve, we derived the maximum elastance, E_{max} and the minimum elastance E_{min}. We then plotted E_{max} and E_{min} with pressure to determine if there was any discernable pattern.

Figure 14 exhibits the relationship between peak pressure and E_{max} for the three vessels. As peak pressure increases, E_{max} increases monotonically for vessel 3. Vessel 3 exhibits a linear relationship (R^2=0.92). The trend is less apparent in the other two vessels.

3.2.3 Mean pressure vs E_{min}

Figure 15 exhibits the relationship between mean pressure and E_{min} for the three vessels. They all show a trend of increasing E_{min} with increase in mean pressure. This trend is consistent, indicated by R^2 values (0.69, 0.97, and 0.85). In vessel 3, there is a significant variation in the E_{min} value.

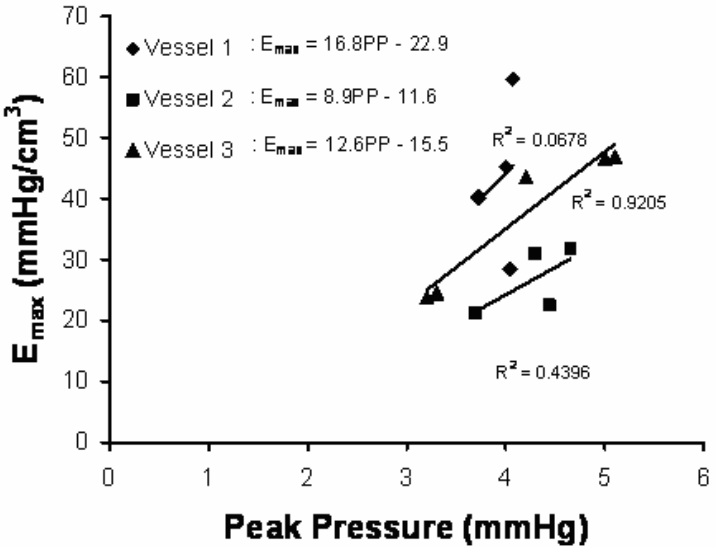

Figure 14: Peak pressure vs E_{max}. E_{max} as a function of peak pressure, the pressure at which E_{max} occurs. We can see that peak pressure and E_{max} are positively correlated. R_2 is the coefficient of determination.

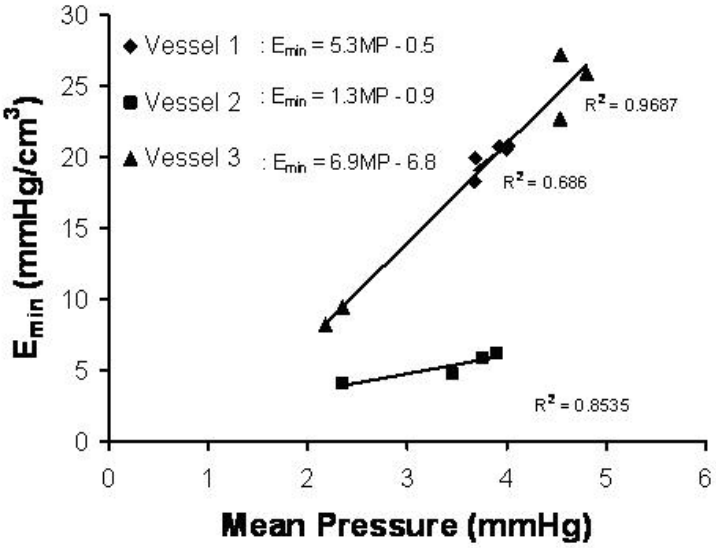

Figure 15: Mean pressure vs E_{min}. E_{min} as a function of mean pressure in three lymphangions. E_{min} increases consistently with mean pressure.

CHAPTER IV

CREATING A DEVICE TO STUDY LYMPHANGION MECHANICS AND FUNCTION

4.1 Experimental set-up

One of the objectives of this thesis is to create a system where the necessary conditions can be automated. In *in vivo* conditions, the lymphangions experience fluctuating preloads and afterloads. Hence we would be controlling the *in vitro* preload and afterload dynamically to mimic conditions *in vivo.*

To do this, the same tubular bath as in Chapter III is used. The flows through the vessel are controlled using a LabVIEW program. The program controls the output of a Reglo digital pump via an RS232 port.

4.2 Protocol for performing isobaric experiments

Isotonic experiments were performed using the set-up explained above. The programming for controlling the pump was done in the LabVIEW programming language. Negative feedback was used to set real-time pressure at a set-point. Figure 16 shows a block diagram representing the equations used for the program.

In these experiments, the transmural pressure was kept constant and the flows were measured for this constant pressure. As the block diagram shows, a pressure was set (P*) and maintained constant using a PI controller. The values for the

constants (K_p and K_i) were chosen after determining the steady state error and then fine-tuning it. The output of the PI controller is a flow signal (Q_s). The pump, connected via an RS232 port, matches this flow, Q, which affects the pressure, P, in the lymphatic vessel, via outflow resistance of the clamp, R. This pressure signal is recorded a strain-gage pressure transducer input into an analog-to-digital converter. The output of the analog-to-digital converter is used as a negative feedback signal for the PI controller. The PI controller keeps increasing or decreasing the pressure (P) till the required pressure is achieved.

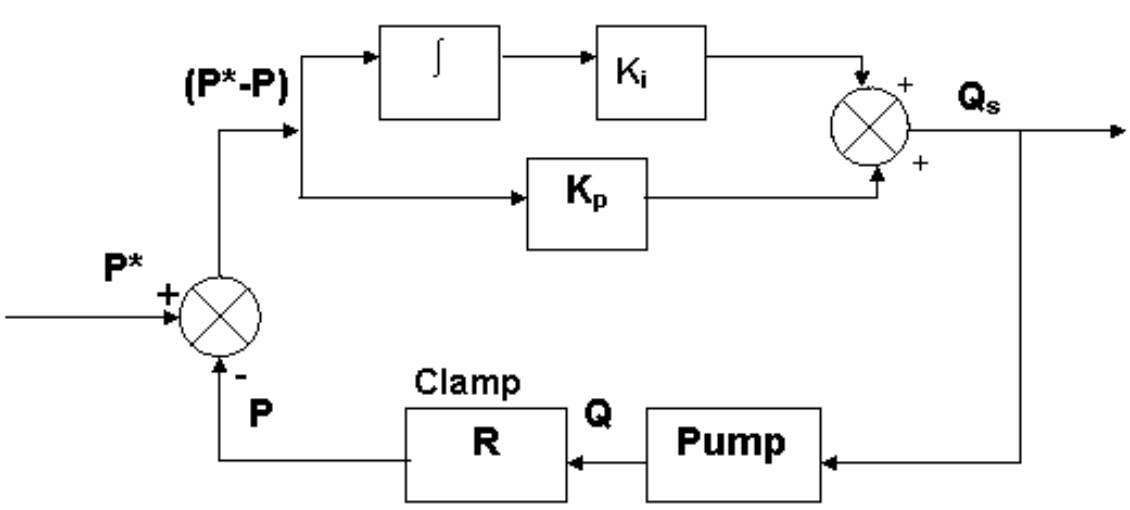

Figure 16: Block diagram for isobaric experiments. P* is the set pressure and P is the real-time pressure. Qs is the flow which comes out of the PI controller.

The following equations are based on the block diagram for the isobaric experiments. The transfer function for the PI controller is:

$$G(s) = K_p + \frac{K_i}{s} \tag{8}$$

We used negative feedback to maintain the real-time pressure equal to a set pressure. The general transfer function for a system with negative feedback is:

$$TF = \frac{G(s)}{1 + H(s)G(s)} \tag{9}$$

From the block diagram we can see that the transfer function of the feedback loop is the product of the output of the pump and the resistance (which is a constant). Thus, the transfer function of the system becomes:

$$\frac{Q_s}{P^*} = \frac{K_i + K_p s}{s + R\left(K_i + K_p s\right)} \tag{10}$$

Figure 17 shows the experimentally-derived pressure vs. pump speed relationship obtained by performing an isobaric experiment on a valveless lymphatic vessel, which did not pump. As the pressure increases, the speed of the pump is also increased, increasing the flow. Hence, as the flow increases, the pressure also increases.

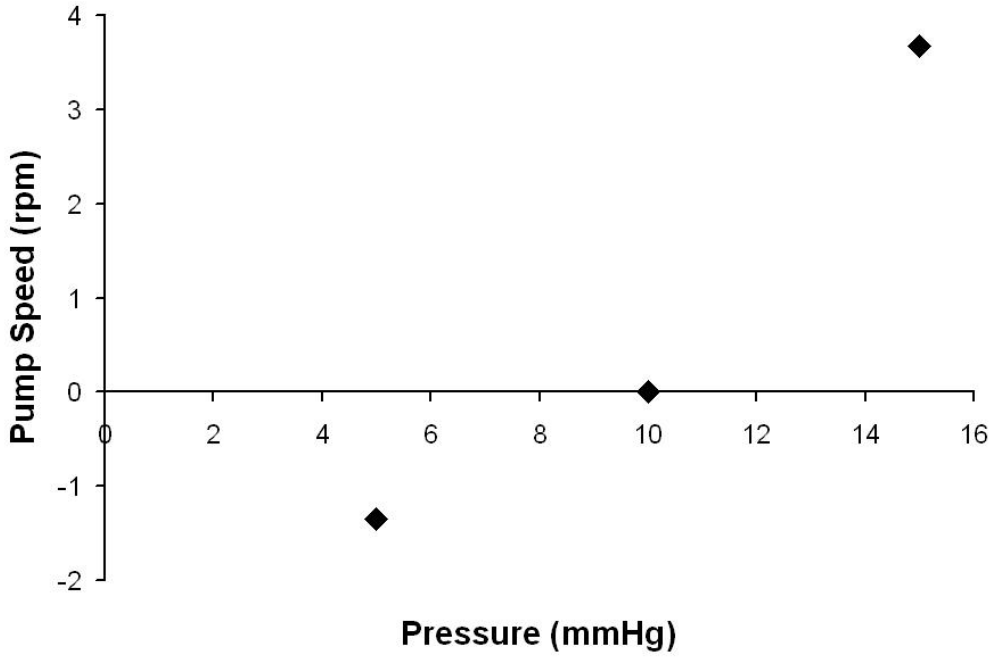

Figure 17: Flow vs pressure plot for isobaric experiments. We can see that as pump speed increased, the resulting pressure increased.

4.3 Protocol for performing isometric experiments

Isometric experiments were performed on the same vessel and in the same tubular bath in which the isobaric experiments were performed. In these experiments, the controller was reconfigured to ensure that pressure was adjusted to keep radius (r*) constant. The block diagram for this is similar to that of the isobaric experiments. Here, the required radius is set (r*). The constants for the PI controller are set by trial and error. A radius tracker program was used to obtain the radius (r) with the help of a Video Dimension Analyzer. Negative feedback was used to set real-time radius at a set-point. Figure 18 shows a block diagram representing the equations used for the programming.

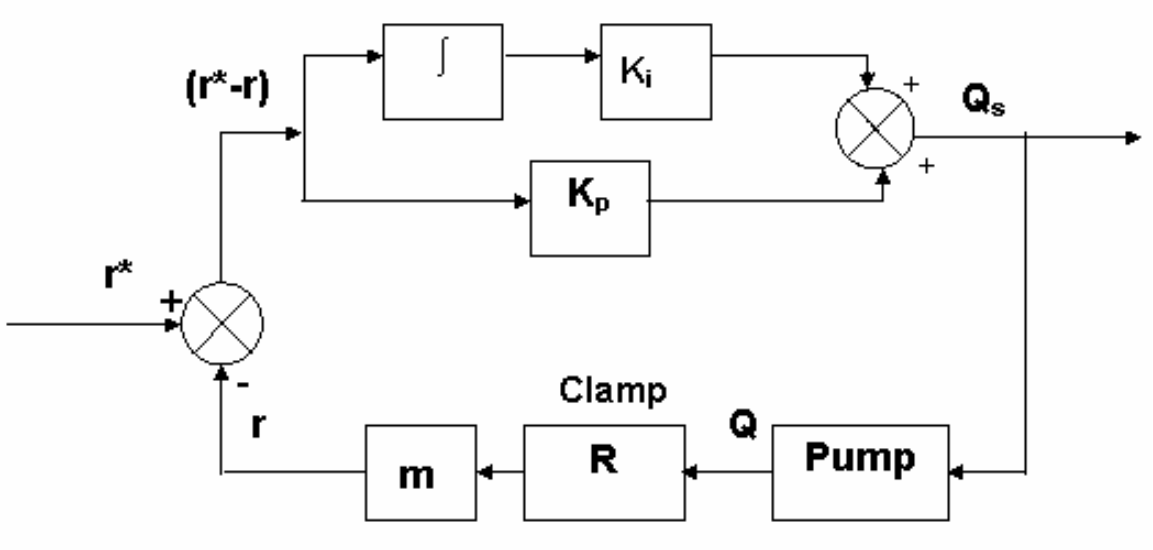

Figure 18: Block diagram for isometric experiments. r* is the set radius and r is the real-time radius that we get from the radius tracker program.

Isometric experiments also use the PI controller. Equation 8 describes the transfer functions for the PI controller, and Eq. 10 describes the system with negative feedback. Similar to the derivation for the isobaric experiment, we can derive a transfer function for the isometric experiments. An additional transfer function (m) is added to relate vessel transmural pressure and radius, assuming a small radius at zero pressure. The transfer function for the isometric experiments becomes:

$$\frac{Q_s}{r^*} = \frac{K_i + K_p s}{s + mR\left(K_i + K_p s\right)} \tag{11}$$

As the block diagram shows, a desired radius (r*) is set. This resulting operation would provide a flow signal (Q_s) which is used to control a pump. The pump provides a flow (Q), causing pressure to change. With a change in pressure, radius is affected.

Similar to figure 17, figure 19 shows the experimental relationship relating pressure and diameter of a non-pumping lymphangion.

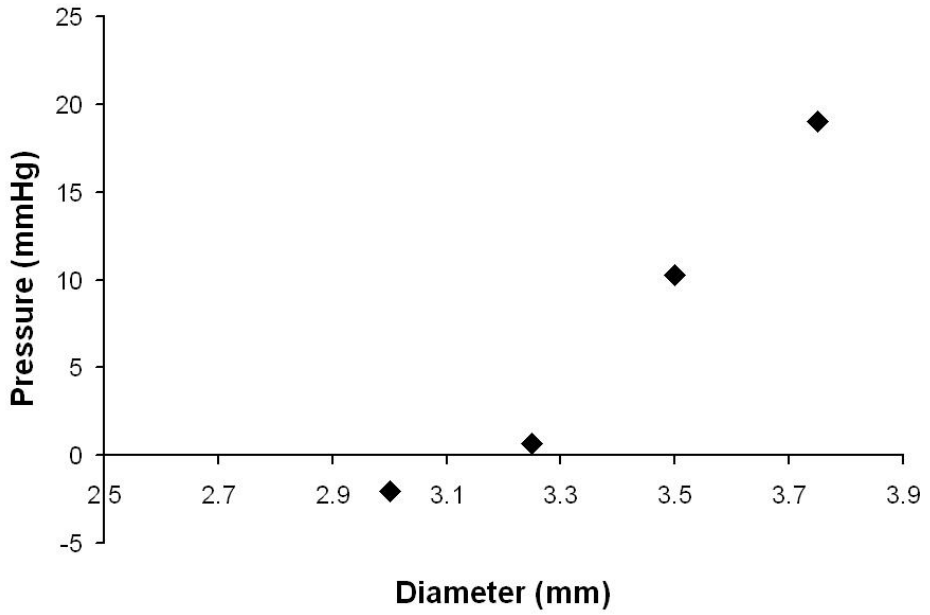

Figure 19: Diameter vs. pressure plot for isometric experiment.

4.4 Protocol for performing isotonic experiments

Isotonic experiments maintain tension at a constant value. Mathematically, tension is the product of pressure and radius, a nonlinear function. As radius decreases, pressure must be increased proportionally. We used the PI control to set a tension (T*) and maintain it at a constant value. The PI controller constants were again chosen according to the method mentioned in the above sections. The radius tracker measured a real-time radius (r) and the pressure transducer measured a real-time pressure (P), the product of which (Pr) yielded real-time wall tension (T). The

set flow signal is converted to a pressure (P) and a radius (r), by the methods stated in the above sections. Figure 20 provides a block diagram for the control of tension.

Figure 21 illustrates the control of tension for various set tensions (T*) in a nonpumping lymphangion. The tensions were set at 5 different values and as we can see, the controlled tension reached the set tension almost immediately. The diameter tracker failed to track radius, leading to a degree of instability.

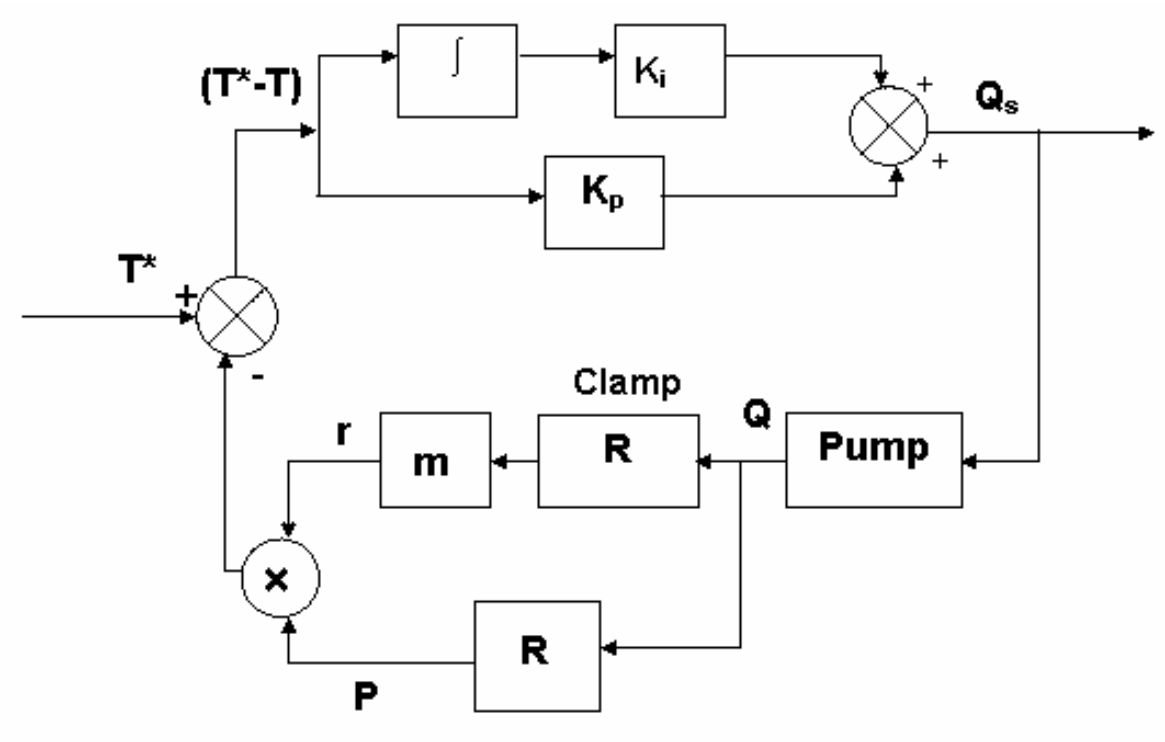

Figure 20: Block diagram for isotonic experiments. T* is the set tension and T is the real-time tension obtained by multiplying real-time pressure and real-time radius.

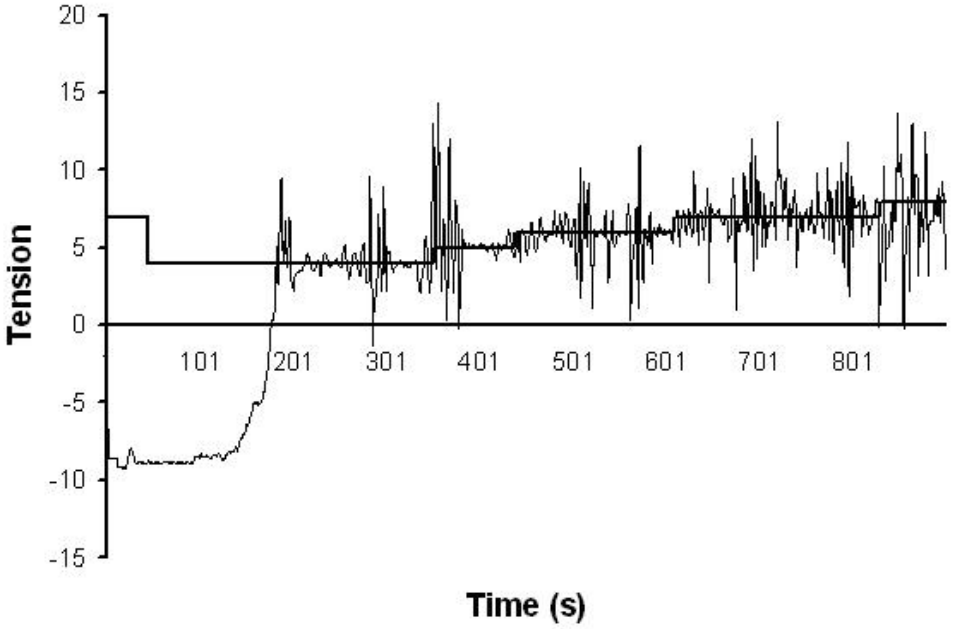

Figure 21: Control of tension. Tensions (in the thick line) were set to several different values and the response of the device (thin line) was noted.

CHAPTER V

ANALYZING THE PERFORMANCE OF THE DEVICE

5.1 Analyzing results for the time-varying elastance concept

The time-varying elastance concept was analyzed and the following limitations were found with the approach:

1) A high degree of variability was found in the contraction of lymphangions, as illustrated by the diverging the elastance curves in Figure 11.
2) The end-diastolic pressure-volume relationship is highly non-linear as shown in Figure 13.
3) Maximum and minimum elastances are sensitive to pressure as shown in Figures 14 and 15.

Due to these limitations in the time-varying elastance curves, these curves were normalized using Eqs. 6 and 7.

The relationship of maximum elastance E_{max} with peak pressure (pressure at which E_{max} occurs) was also studied. In two vessels, the value of E_{max} increased monotonically with an increase in pressure, suggesting that the lymphangion contracts disproportionately harder at higher pressures.

The relationship between E_{min} and mean pressure was also studied. It was found that E_{min} increased as mean pressure increased. This may be due to the high degree of non-linearity in the end-diastolic pressure-volume relationship. In some

vessels, there was as much as five times increase in E_{min} as mean pressure increased as shown in figure 15.

5.2 Analyzing the frequency response of the device

A device was created to study lymphangion function and mechanics. Isometric, isotonic and isobaric experiments were performed using this device. To ensure that the device can respond fast enough to regulate pressure, radius, and tension, frequency response plots were obtained. A sinusoidal input was given to the device at various frequencies and the resulting *amplitude ratio* (actual amplitude/set amplitude) was calculated and plotted against frequencies. Such plots were obtained for different set amplitudes as shown in the figures 22-24.

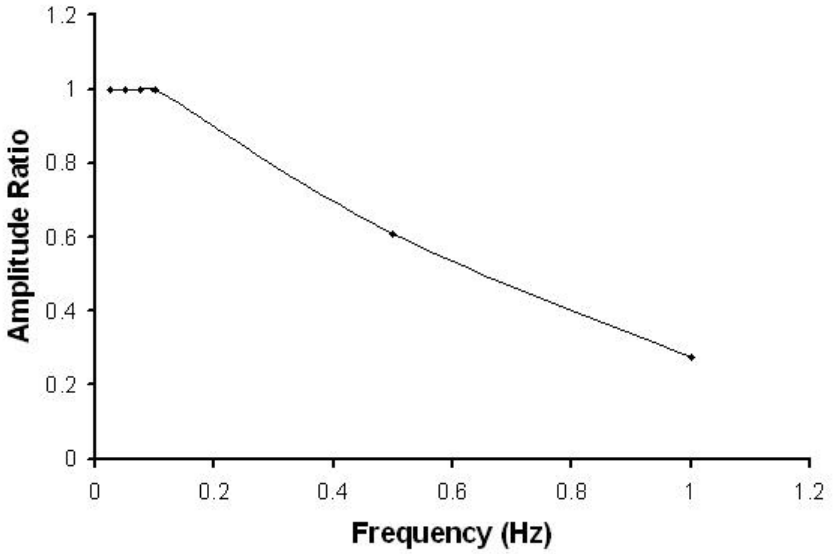

Figure 22: Frequency response plot for a set amplitude of 1mm diameter. The diameter varied between 4 and 6 mm.

The frequency response plots showed that the system gives good response for frequencies of 0.005-0.5 Hz. The device works well for the frequencies expected for pumping lymphangions.

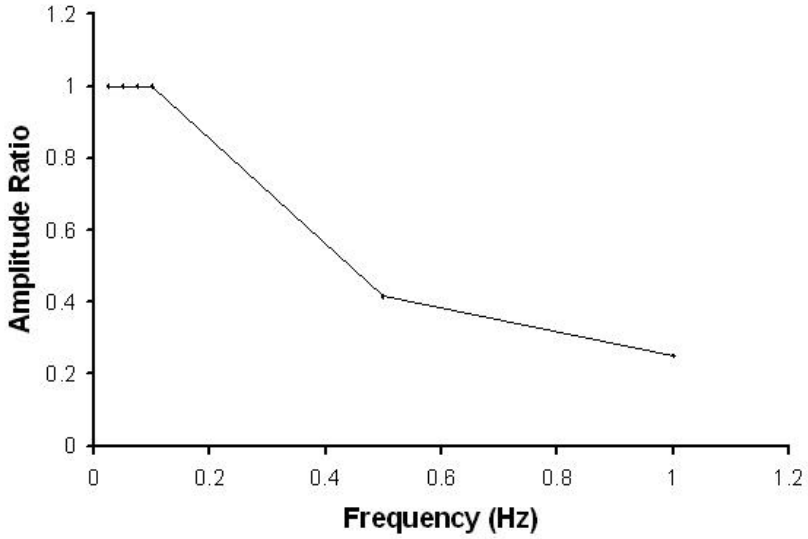

Figure 23: Frequency response plot for a set amplitude of 1.5mm diameter. The diameter varied between 3.5 and 6.5 mm.

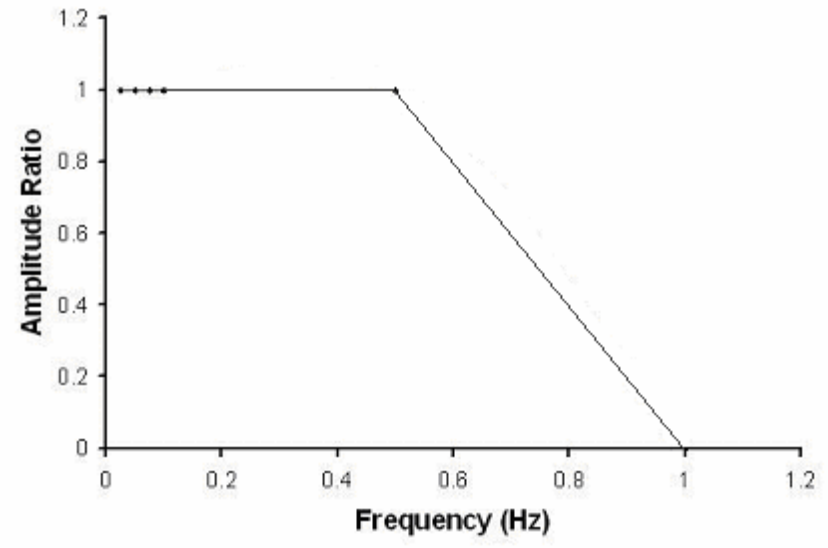

Figure 24: Frequency response plot for a set amplitude of 0.5mm diameter. The diameter varied between 4.5 and 5.5 mm.

CHAPTER VI

SUMMARY

6.1 Applicability of the time-varying elastance concept on lymphangions

As described in chapter I, the time-varying elastance description is a common way to characterize ventricular behavior independent of preload and afterload, and its maximum value, E_{max}, has become a common index of contractility. One of our objectives was to test if this concept applied to lymphangions as well. The analysis of the results obtained from the experiments suggested that time-varying elastance concept could be used as a contractility index, but with major modifications. According to the original formulation (19), the time-varying elastance of the heart is relatively stable and insensitive to preload and afterload. Although the three limitations explained in chapter V also apply to ventricular elastance, they are even more pronounced in cyclically contracting lymphatic vessels. Deviations of lymphangion behavior from the classic formulation of the time-varying elastance (Eq. 1), however, may be quantifiable and predictable.

This high degree of variability may also be due to the fundamental differences of lymphangions and ventricles. Lymphangions not only act like pumping ventricles, they also act like muscular blood vessels in that they have a variable resting tone. That is, in diastole, lymphatic smooth muscle is not completely relaxed. Whereas E_{max} has been used as an index of contraction, E_{min} might be used as an index of

relaxation. Characterizing E_{min} with flow may be a fruitful area of exploration, particularly given the recent studies of Gashev and Zaweija (9).

The present work reports preliminary data obtained from only three vessels. To corroborate the results obtained here, there is a need to study a larger number of vessels. Furthermore, for a more balanced picture, it is imperative to characterize the differences in large and small lymphangions, which have been shown to respond to edemagenic stress differently (2). There may also be fundamental differences in lymphatic vessels taken from different parts of the lymphatic network (2, 10). The present work, however, provides a device and methodology to lay the groundwork for future studies, and clearly suggests that, if used with caution, the time-varying elastance concept may be applied to describe lymphatic function.

Understanding when and how the lymphangions contract and relax can elucidate the mechanical factors affecting lymph flow. A simple, data-based characterization of lymphangion contraction that predicts its reaction to changes in its mechanical environment can be used to construct models. An analytical description of the normalized elastance curves (figure 3), modified by E_{min} or E_{max} expressed as function of pressure and flow, may provide a more solid basis for use in modeling lymphatic vessels (7, 22). Just as the lymphangion is the fundamental building block of the lymphatic system, this simple description of a lymphangion has the potential to form a fundamental building block of a large-scale lymphatic system model.

6.2 Analysis of the lymphatic vessel function and lymphangion mechanics

Isobaric, isometric and isotonic experiments were performed on a lymphatic vessel and the results obtained have been shown in chapter IV. As explained in chapter IV, isobaric experiments are performed by keeping the pressure constant. Performing isobaric experiments, gives yields the relationship between axial pressure gradient and flow. This information, of how flows change with changes in pressure, is useful for analyzing the lymphangion function.

The above information can be supplemented by isometric experiments. In isometric experiments, radius is maintained constant. Performing the isometric experiments yields us the maximum tension exerted on the lymphatic vessel. To obtain this information, the radius was plotted against pressure. Classical isometric and isotonic experiments on the cardiac muscle have been described in chapter I. Our experiments however, were performed in a tubular bath, and so the setting is different from the classical experiments. Instead of a strip of muscle, the intact vessel preserves the original geometry.

Isometric and isotonic experiments together can describe vessel mechanics. For isotonic experiments, tension was held constant. Real-time tension was obtained as a product of pressure and radius. An isotonic experiment has been performed on an intact, inflated lymphatic vessel for the first time, and we have been successful in maintaining a set tension on the vessel as shown in figure 21. There have been a few problems due to the diameter tracking program, in maintaining a constant radius and thus tension, but these issues can be easily solved to help maintain a set tension. The

tools have thus been developed to fully characterize fundamental lymphatic mechanics.

REFERENCES

1. **Benoit JN.** Relationships between lymphatic pump flow and total lymph flow in the small intestine. *Am J Physiol* 261: H1970-1978, 1991.
2. **Benoit JN, Zawieja DC, Goodman AH, and Granger HJ.** Characterization of intact mesenteric lymphatic pump and its responsiveness to acute edemagenic stress. *Am J Physiol* 257: H2059-2069, 1989.
3. **Brady AJ.** The three element model of muscle mechanics: its applicability to cardiac muscle. *Physiologist* 10: 75-86, 1967.
4. **Drake R, Giesler M, Laine G, Gabel J, and Hansen T.** Effect of outflow pressure on lung lymph flow in unanesthetized sheep. *J Appl Physiol* 58: 70-76, 1985.
5. **Drake RE, Adcock DK, Scott RL, and Gabel JC.** Effect of outflow pressure upon lymph flow from dog lungs. *Circ Res* 50: 865-869, 1982.
6. **Drake RE and Gabel JC.** Effect of outflow pressure on liver lymph flow in unanesthetized sheep. *Am J Physiol* 259: R780-785, 1990.
7. **Drake RE, Weiss D, and Gabel JC.** Active lymphatic pumping and sheep lung lymph flow. *J Appl Physiol* 71: 99-103, 1991.
8. **Frank O.** Die Grundform des Arteriellen Pulses. *ZBiol* 37: 483-526, 1899.
9. **Gashev AA, Davis MJ, Delp MD, and Zawieja DC.** Regional variations of contractile activity in isolated rat lymphatics. *Microcirculation* 11: 477-492, 2004.

10. **Gashev AA, Davis MJ, and Zawieja DC.** Inhibition of the active lymph pump by flow in rat mesenteric lymphatics and thoracic duct. *J Physiol* 540: 1023-1037, 2002.

11. **Gashev AA and Zawieja DC.** Physiology of human lymphatic contractility: a historical perspective. *Lymphology* 34: 124-134, 2001.

12. **Hill AV.** The heat of shortening and dynamic constants of muscle. *R. Soc. London* (1938 ed.), 1938, p. 136.

13. **Li B, Silver I, Szalai JP, and Johnston MG.** Pressure-volume relationships in sheep mesenteric lymphatic vessels in situ: response to hypovolemia. *Microvasc Res* 56: 127-138, 1998.

14. **Noordergraaf A.** *Circulatory System Dynamics*: New York: Academic Press Inc., 1978.

15. **Palladino J MJ, and Noordergraaf A.** Defining ventricular elastance. *Proceedings of the 20th Annual International Conference of the IEEE, Hong Kong*, 1998, p. 383 - 386.

16. **Parmley WW and Sonnenblick EH.** Series elasticity in heart muscle. Its relation to contractile element velocity and proposed muscle models. *Circ Res* 20: 112-123, 1967.

17. **Sagawa K, Suga H, Shoukas AA, and Bakalar KM.** End-systolic pressure/volume ratio: a new index of ventricular contractility. *Am J Cardiol* 40: 748-753, 1977.

18. **Schmid-Schonbein GW.** Microlymphatics and lymph flow. *Physiol Rev* 70: 987-1028, 1990.

19. **Suga H and Sagawa K.** Instantaneous pressure-volume relationships and their ratio in the excised, supported canine left ventricle. *Circ Res* 35: 117-126, 1974.

20. **Suga H, Sagawa K, and Shoukas AA.** Load independence of the instantaneous pressure-volume ratio of the canine left ventricle and effects of epinephrine and heart rate on the ratio. *Circ Res* 32: 314-322, 1973.

21. **Nichols WW and O'Rourke MF.** *McDonald's Blood Flow in Arteries*: New York: Oxford University Press, 1998.

22. **Zawieja D BJ, and Granger HJ.** Coordination of lymphatic pumping. A theoretical model (Abstract). *Federation Proc*, 1987, p. 1546.

VITA

Name:	Shruti Rajagopalan
Date of birth:	Oct 21, 1980.
Address:	400 Second Street, Apt 'B' College Station, TX-77840.
Education:	
2002-2004	Texas A&M University Master of Science Biomedical Engineering, 2004.
1998-2002	Sathyabama Engineering College Madras University Chennai, India. Bachelor of Engineering, Electronics & Instrumentation Engineering, 2002.